

Supporting Information

Facile Fabrication of Sandwich Structured WO₃ Nanoplate Arrays for Efficient Photoelectrochemical Water Splitting

Xiaoyang Feng, Yubin Chen, Zhixiao Qin, Menglong Wang and Liejin Guo**

International Research Center for Renewable Energy, State Key Laboratory of Multiphase Flow in Power Engineering, Xi'an Jiaotong University, Shaanxi 710049, P. R. China.

E-mail: ybchen@mail.xjtu.edu.cn (Y. Chen); lj-guo@mail.xjtu.edu.cn (L. Guo).

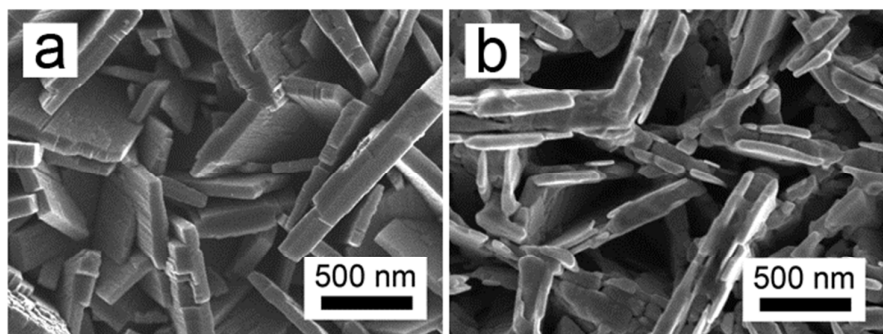


Figure S1. SEM images of (a) the hydrothermally prepared $\text{WO}_3 \cdot 0.33\text{H}_2\text{O}$ film and (b) the corresponding WO_3 annealed at 500 °C.

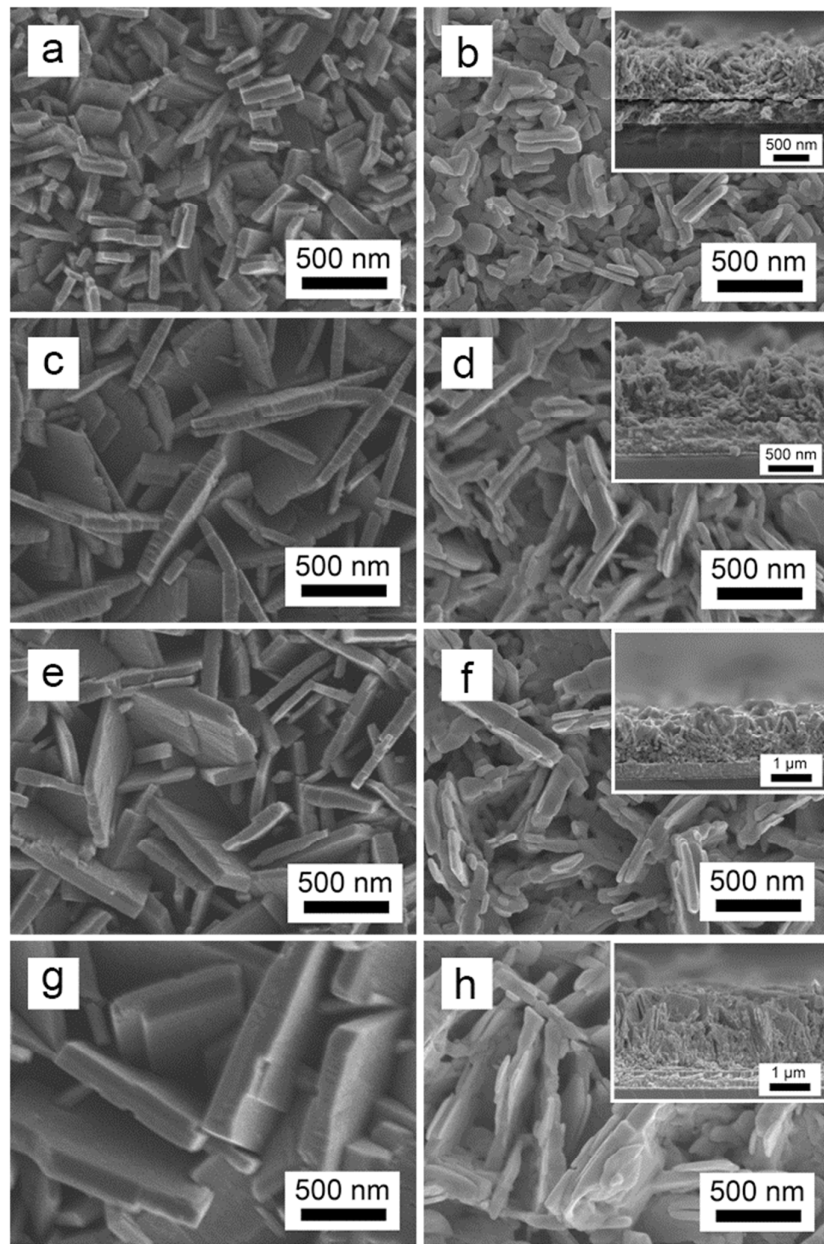


Figure S2. SEM images of $\text{WO}_3 \cdot 0.33\text{H}_2\text{O}$ films hydrothermally prepared for varied time and the corresponding WO_3 annealed at 500 °C. (a, b) 2 h, (c, d) 3 h, (e, f) 4 h, and (g, h) 6 h. Insets show the corresponding cross-section images of annealed samples.

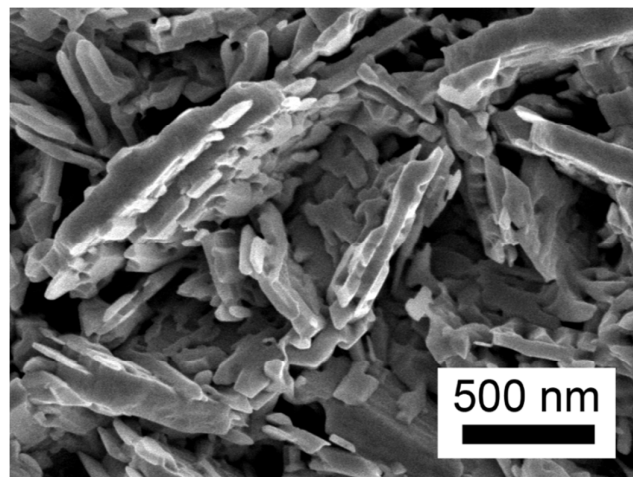


Figure S3. SEM image of the corresponding WO_3 by annealing the powder scraped from the as-prepared $\text{WO}_3 \cdot 0.33\text{H}_2\text{O}$ film at 500 °C for 1 h.

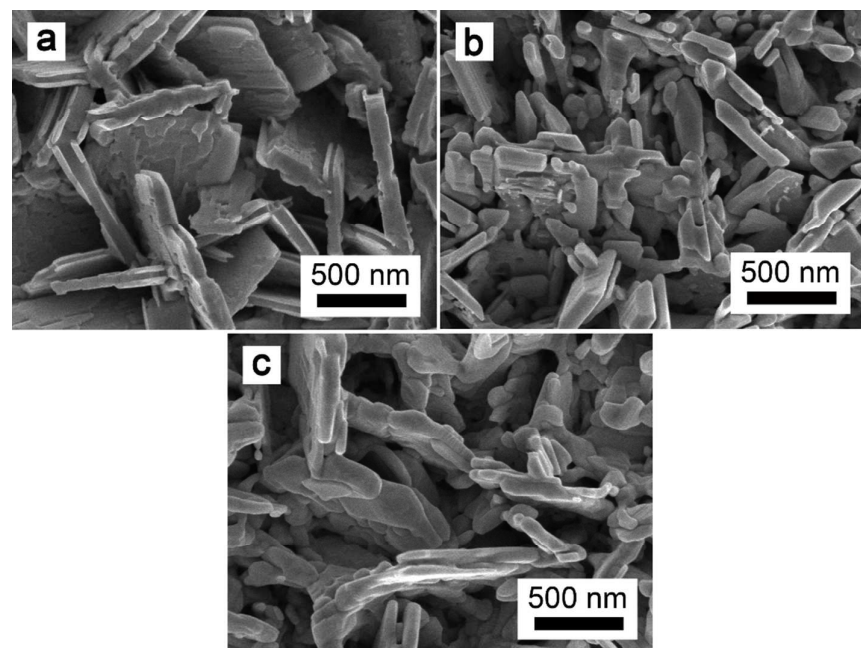


Figure S4. SEM images of WO_3 films annealed at 500 °C for (a) 0.5 h, (b) 3 h, and (c) 5 h.

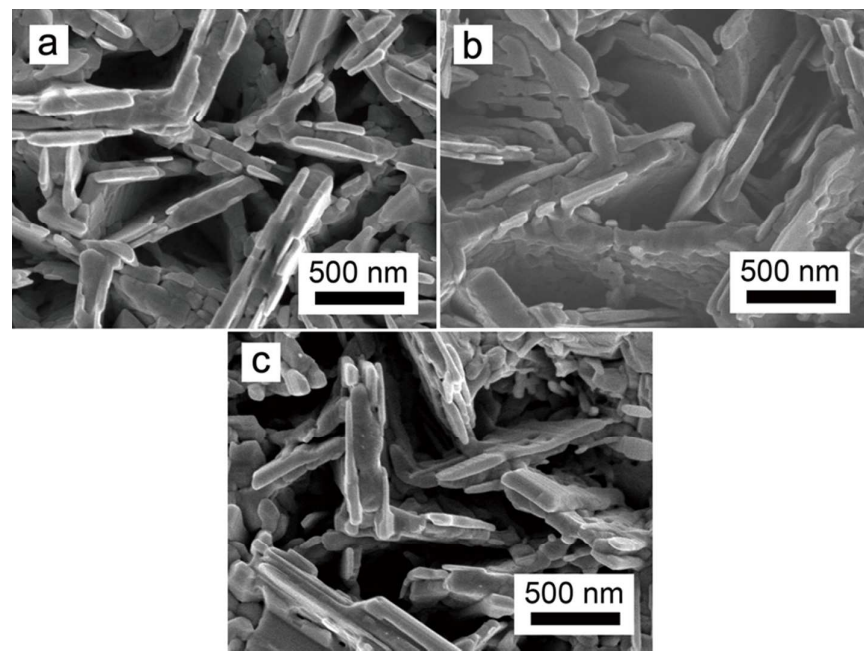


Figure S5. SEM images of WO₃ films annealed at 500 °C for 1 h using different heating rates: (a) 6 °C/min, (b) 4 °C/min, and (c) 3 °C/min.

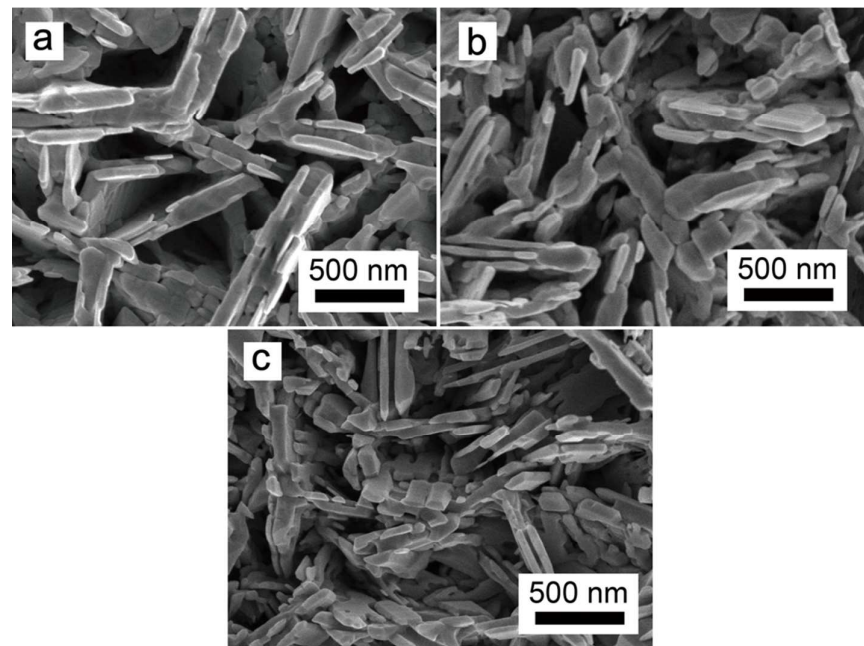


Figure S6. SEM images of WO₃ films annealed at 500 °C for 1 h using different cooling rates: (a) 2.5 °C/min, (b) 3.5 °C/min, and (c) 5 °C/min.

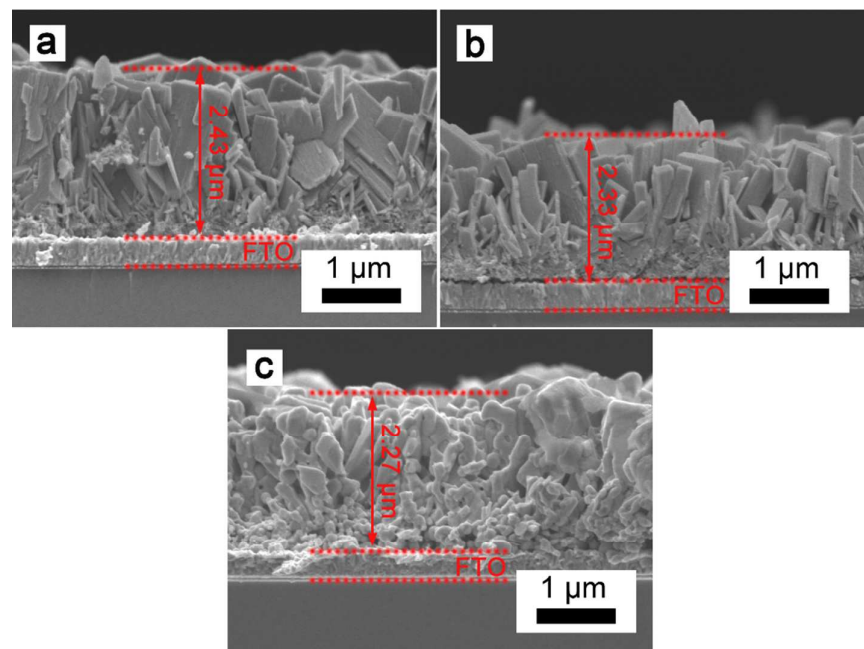


Figure S7. Cross-section SEM images of as-prepared films (a) before and after annealing at (b) 400 °C and (c) 600 °C.

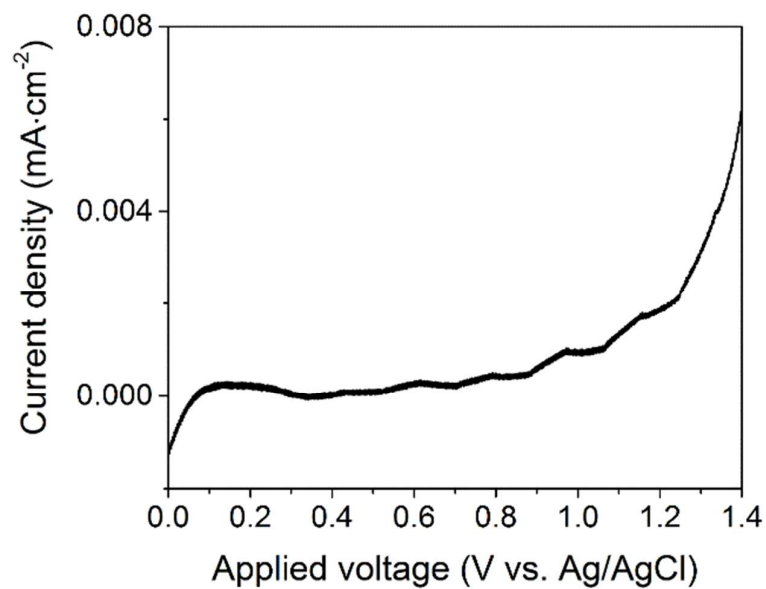


Figure S8. Linear sweep voltammetry of as-prepared $\text{WO}_3 \cdot 0.33\text{H}_2\text{O}$ photoanode under incident chopped light.

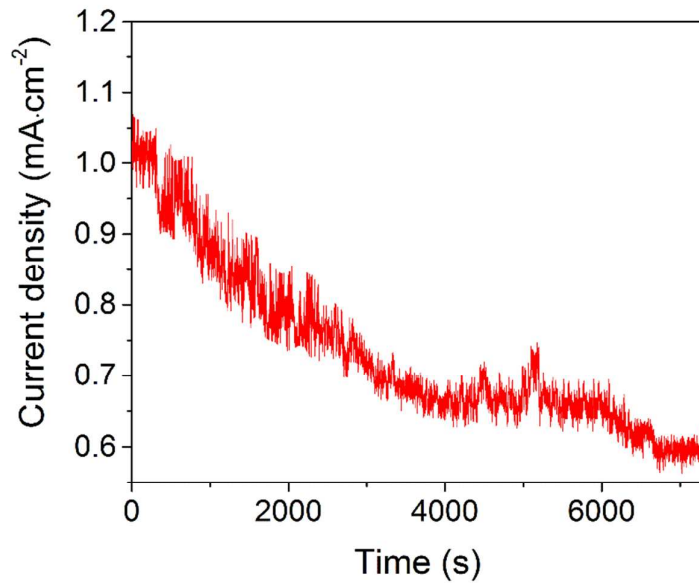


Figure S9. Photocurrent-time plot (at 0.6 V vs. Ag/AgCl) over the sandwich structured WO_3 photoanode in a three-electrode cell under simulated sunlight.

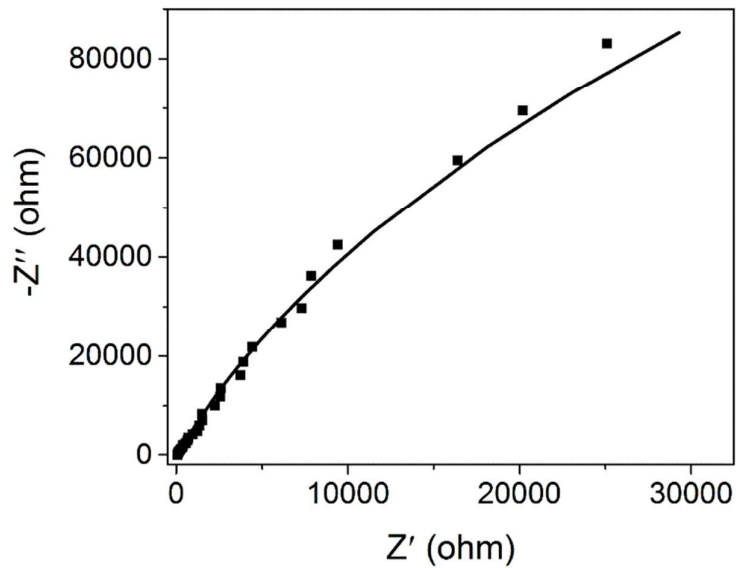


Figure S10. Nyquist experimental data and fitting plot of as-prepared $\text{WO}_3 \cdot 0.33\text{H}_2\text{O}$ photoanode.

Table S1. An overview of representative WO_3 photoanodes reported for efficient photoelectrochemical water splitting.

Fabrication method	Morphology	Electrolyte (light source)	$J (\text{mA}\cdot\text{cm}^{-2})$ (applied potential)	IPCE (%) at 400 nm (applied potential)	Ref.
Hydrothermal	Nanorod	0.5 M Na_2SO_4 (AM 1.5 G)	1.05 (1.1 V vs. SCE)	\	1
Hydrothermal	Nanorod	0.5 M Na_2SO_4 (AM 1.5 G)	2.26 (1.23 V vs. RHE)	35 (0.8 V vs. Ag/AgCl)	2
Hydrothermal	Nanoplate	0.5 M Na_2SO_4 (AM 1.5 G)	0.25 (1.23 V vs. RHE)	\sim 11 (1.0 V vs. Ag/AgCl)	3
Hydrothermal	Plate-like	0.5 M H_2SO_4 (Xe lamp)	4.13 (1.6 V vs. Ag/AgCl)	\	4
Hydrothermal	Nanoflower	1 M H_2SO_4 (AM 1.5 G)	\sim 1.25 (1.2 V vs. SCE)	29 (0.8 V vs. SCE)	5
Hydrothermal	Nanoflake	1 M H_2SO_4 (AM 1.5 G)	\sim 1.1 (1.0 V vs. Ag/AgCl)	\sim 15 (1.0 V vs. Ag/AgCl)	6
PLD	Nano-tree	1 M H_2SO_4 (AM 1.5 G)	1.85 (0.8 V vs. RHE)	63 (1.0 V vs. RHE)	7
PLD	Tree-like	0.5 M phosphate buffer (AM 1.5 G)	1.8 (1.23 V vs. RHE)	\sim 50 (1.23 V vs. RHE)	8
Solvothermal	Flake-wall structure	0.1 M Na_2SO_4 (Xe lamp)	\sim 1.85 (1.2 V vs. Ag/AgCl)	36 (1.2 V vs. Ag/AgCl)	9
Solvothermal	Nano-multilayer	0.1 M Na_2SO_4 (AM 1.5 G)	1.62 (1.25 V vs. Ag/AgCl)	25 (1.27 V vs. RHE)	10
Anodization	Nanorod/nanoflake	phosphate buffer	0.9 (1.2 V vs. RHE)	\sim 28 (1.0 V vs. RHE)	11
	nano particle/triple-layer	pH = 7 (Xe lamp)			
Anodization	Nanoporous	0.5 M H_2SO_4 (Xe lamp)	3.45 (1.6 V vs. Ag/AgCl)	20 (1.2 V vs. Ag/AgCl)	12
Anodization	Nanocrystal	1 M H_2SO_4 (AM 1.5 G)	3.5 (1.5 V vs. SCE)	45 (1.5 V vs. SCE)	13
Sol-gel	Nanoparticle	3 M H_2SO_4 (AM 1.5 G)	2.7 (1 V vs. RHE)	43 (0.5 V vs. MSE)	14
Colloid deposition	Nanoparticle	1 M H_2SO_4 (Xe lamp)	3.7 (1.3 V vs. Ag/AgCl)	\	15
Colloid deposition	Nanowire	0.5 M H_2SO_4 (AM 1.5 G)	1.96 (1.23 V vs. RHE)	\sim 50 (1.23 V vs. RHE)	16

Polystyrene colloid templates	Inverse opal	1 M H ₂ SO ₄ (Xe lamp)	0.95 (1.2 V vs. Ag/AgCl)	\	17
Reactive magnetron sputtering	Nanocrystal	0.5 M NaClO ₄ (Mercury-Xe lamp)	2.5 (1.0 V vs. Ag/AgCl)	\	18
Hydrothermal	Nanoplate	0.5 M Na ₂ SO ₄ (AM 1.5 G)	1.88 (1.3 V vs. Ag/AgCl)	65 (1.0 V vs. Ag/AgCl)	This work

SCE: saturated calomel electrode; RHE: reversible hydrogen electrode; MSE: mercurous sulfate electrode.

REFERENCES

- (1) Liu, Y.; Zhao, L.; Su, J. Z.; Li, M. T.; Guo, L. J., Fabrication and Properties of a Branched (NH₄)_(x)WO₃ Nanowire Array Film and a Porous WO₃ Nanorod Array Film. *ACS Appl. Mater. Interfaces* **2015**, *7*, 3532-3538.
- (2) Kalanur, S. S.; Hwang, Y. J.; Chae, S. Y.; Joo, O. S., Facile Growth of Aligned WO₃ Nanorods on FTO Substrate for Enhanced Photoanodic Water Oxidation Activity. *J. Mater. Chem. A* **2013**, *1*, 3479-3488.
- (3) Zheng, J. Y.; Song, G.; Hong, J. S.; Van, T. K.; Pawar, A. U.; Kim, D. Y.; Kim, C. W.; Haider, Z.; Kang, Y. S., Facile Fabrication of WO₃ Nanoplates Thin Films with Dominant Crystal Facet of (002) for Water Splitting. *Cryst. Growth. Des.* **2014**, *14*, 6057-6066.
- (4) Yang, J.; Li, W. Z.; Li, J.; Sun, D. B.; Chen, Q. Y., Hydrothermal Synthesis and Photoelectrochemical Properties of Vertically Aligned Tungsten Trioxide (Hydrate) Plate-Like Arrays Fabricated Directly on FTO Substrates. *J. Mater. Chem.* **2012**, *22*, 17744-17752.

- (5) Wang, N.; Wang, D. G.; Li, M. R.; Shi, J. Y.; Li, C., Photoelectrochemical Water Oxidation on Photoanodes Fabricated with Hexagonal Nanoflower and Nanoblock WO_3 . *Nanoscale* **2014**, *6*, 2061-2066.
- (6) Li, W. J.; Da, P. M.; Zhang, Y. Y.; Wang, Y. C.; Lin, X.; Gong, X. G.; Zheng, G. F., WO_3 Nanoflakes for Enhanced Photoelectrochemical Conversion. *ACS Nano* **2014**, *8*, 11770-11777.
- (7) Balandeh, M.; Mezzetti, A.; Tacca, A.; Leonardi, S.; Marra, G.; Divitini, G.; Ducati, C.; Meda, L.; Di Fonzo, F., Quasi-1D Hyperbranched WO_3 Nanostructures for Low-Voltage Photoelectrochemical Water Splitting. *J. Mater. Chem. A* **2015**, *3*, 6110-6117.
- (8) Shin, S.; Han, H. S.; Kim, J. S.; Park, I. J.; Lee, M. H.; Hong, K. S.; Cho, I. S., A Tree-Like Nanoporous WO_3 Photoanode with Enhanced Charge Transport Efficiency for Photoelectrochemical Water Oxidation. *J. Mater. Chem. A* **2015**, *3*, 12920-12926.
- (9) Amano, F.; Li, D.; Ohtani, B., Fabrication and Photoelectrochemical Property of Tungsten (VI) Oxide Films with a Flake-Wall Structure. *Chem. Commun.* **2010**, *46*, 2769-2771.
- (10) Zhang, J. J.; Zhang, P.; Wang, T.; Gong, J. L., Monoclinic WO_3 Nanomultilayers with Preferentially Exposed (002) Facets for Photoelectrochemical Water Splitting. *Nano Energy* **2015**, *11*, 189-195.
- (11) Qi, H.; Wolfe, J.; Wang, D. P.; Fan, H. J.; Fichou, D.; Chen, Z., Triple-Layered Nanostructured WO_3 Photoanodes with Enhanced Photocurrent Generation and

Superior Stability for Photoelectrochemical Solar Energy Conversion. *Nanoscale* **2014**, *6*, 13457-13462.

(12) Li, W.; Li, J.; Wang, X.; Luo, S.; Xiao, J.; Chen, Q., Visible Light Photoelectrochemical Responsiveness of Self-Organized Nanoporous WO_3 Films. *Electrochim. Acta* **2010**, *56*, 620-625.

(13) Cristino, V.; Caramori, S.; Argazzi, R.; Meda, L.; Marra, G. L.; Bignozzi, C. A., Efficient Photoelectrochemical Water Splitting by Anodically Grown WO_3 Electrodes. *Langmuir* **2011**, *27*, 7276-7284.

(14) Hilaire, S.; Suess, M. J.; Kranzlin, N.; Bienkowski, K.; Solarska, R.; Augustynski, J.; Niederberger, M., Microwave-Assisted Nonaqueous Synthesis of WO_3 Nanoparticles for Crystallographically Oriented Photoanodes for Water Splitting. *J. Mater. Chem. A* **2014**, *2*, 20530-20537.

(15) Kim, J. K.; Shin, K.; Cho, S. M.; Lee, T.-W.; Park, J. H., Synthesis of Transparent Mesoporous Tungsten Trioxide Films with Enhanced Photoelectrochemical Response: Application to Unassisted Solar Water Splitting. *Energy Environ. Sci.* **2011**, *4*, 1465.

(16) Goncalves, R. H.; Leite, L. D. T.; Leite, E. R., Colloidal WO_3 Nanowires as a Versatile Route to Prepare a Photoanode for Solar Water Splitting. *Chemsuschem* **2012**, *5*, 2341-2347.

(17) Kim, J. K.; Moon, J. H.; Lee, T. W.; Park, J. H., Inverse Opal Tungsten Trioxide Films with Mesoporous Skeletons: Synthesis and Photoelectrochemical Responses. *Chem. Commun.* **2012**, *48*, 11939-11941.

(18) Vidyarthi, V. S.; Hofmann, M.; Savan, A.; Sliozberg, K.; König, D.; Beranek, R.;

Schuhmann, W.; Ludwig, A., Enhanced Photoelectrochemical Properties of WO_3 Thin Films Fabricated by Reactive Magnetron Sputtering. *Int. J. Hydrogen Energy* **2011**, *36*, 4724-4731.